Dynamics of a charged Ne atom near graphene edges under a positive static electric field

Yanlin Gao*, Susumu Okada

Department of Physics, Graduate School of Pure and Applied Sciences, University of Tsukuba, 1-1-1 Tennodai, Tsukuba, Tsukuba 305-8571, Japan

Abstract

Using the density functional theory combined with the effective screening medium method, the dynamical properties of a Ne atom near graphene edges under an external electric field are investigated. The field-induced motions of a Ne atom near the graphene edges are sensitive to the initial position of Ne and the edge morphology of graphene. The Ne atom is attracted to the edge atomic sites of graphene when it is initially located above the edges. The Ne atom moves to the counter negative electrode when it is located alongside the armchair edge. The Ne atom approximately maintains its initial position when it is located alongside the zigzag edge owing to the polarity of the Ne atom induced by the edge morphology.

1. Introduction

Ever since the successful synthesis of graphene [1, 2, 3, 4, 5], graphene has been extensively studied as an emerging material in the pure and applied sciences. Graphene provides an ultimate two-dimensional electron system, which causes unusual physical phenomena associated with its dimensionality and makes it applicable for a wide range of modern technologies. Conical dispersion bands at the Fermi level, which arise from itinerant π electrons on the honeycomb covalent networks, endow graphene with a remarkable carrier mobility of

*Corresponding author
Email address: ylgao@comas.frsc.tsukuba.ac.jp (Yanlin Gao)

up to 100,000 $cm^2V^{-1}s^{-1}$, although graphene has a vanishing density of state at the Fermi level [6, 7, 8]. The conical dispersion band at the Fermi level leads to a further variation in the electronic structure of graphene derivatives, which is absent in pristine graphene. Graphene nanoribbons are representative examples of such derivatives. Graphene nanoribbons with zigzag edges have peculiar edge localized states, which induce spin polarization because of the delicate balance of the electron transfer around the edge atomic sites [19, 20, 21, 22]. In contrast, graphene nanoribbons with armchair edges are semiconductors, whose band gap asymptotically decreases with the increase of their width and oscillates in triple periodicity of its ribbon width. The ribbons with chiral edges possess a localized state at the edge with the zigzag portions [23]. In addition to graphene nanoribbons, graphene with periodic pores is another example. The periodic pores in graphene cause a flat dispersion band at the Fermi level or kagome bands around the Fermi level owing to the symmetry breaking of the graphene honeycomb network [24, 25].

Because the electronic structure of graphene and its derivatives are sensitive to their geometric structures, precise structure characterization is essential for their scientific investigations and technological applications. Microscopic techniques are commonly used to determine their geometric structures on the atomic-scale. Scanning tunneling microscopy, transmission electron microscopy, and field electron microscopy are known to provide atomic information on graphene and graphene nanostructures [26, 27, 28, 29, 30, 31, 32, 33]. In addition, field ion microscopy (FIM) is another possible procedure to determine the atomic structure of nanomaterials and the surfaces of bulk materials. In FIM, rare-gas atoms introduced near the surface and tip of the samples result in atomic-resolution images on the screen after being ionized and then accelerated by a strong positive electric field. Several FIM experiments have provided atomic-scale images of carbon nanostructures, such as carbon nanotubes [35, 34], monatomic carbon chains [36], and graphene [37]. Although FIM can provide atomic-resolution images of carbon nanostructures, the microscopic dynamics of rare-gas atoms around the carbon nanostructures under a positive electric

field have not been addressed to date, which is in sharp contrast to the other microscopy procedures [38, 41, 40, 39]. Therefore, in this work, we aim to investigate the dynamical properties of a Ne atom located around graphene edges under a positive electric field, in terms of the edge shapes of graphene and an initial position of Ne atom. Based on the density functional theory (DFT) with the effective screening medium (ESM) method, we provide theoretical insight into the physics associated with the FIM of graphene nano structures. Our first-principles molecular dynamics (MD) simulations show that the dynamics of a Ne atom around the graphene edges strongly depend on the edge morphologies associated with the polarization on both the graphene edges and Ne atoms by the positive electric field.

2. Calculation methods

All calculations were based on DFT [42, 43] implemented in the program package STATE [44]. The exchange-correlation potential among interacting electrons was treated using the local density approximation (LDA) with the Perdew-Zunger functional [45, 46], because LDA is known to qualitatively reproduce the binding properties of a non-covalent interaction [47]. The interaction between electrons and ions was described by the ultrasoft pseudopotentials generated by the Vanderbilt scheme [48]. The valence wave function and deficit charge densities were expanded in terms of the plane-wave basis sets with cut-off energies of 25 and 225 Ry, respectively. First-principles MD simulations were conducted using the velocity scaling method to maintain the temperature at 100 and 1000 K during the simulations.

3. Structure model

In this work, to investigate the dynamics of Ne around graphene edges under a positive electric field by simulating the initial microscopic process of FIM of the graphene edge, we considered an armchair graphene nanoribbon (AGNR) and a zigzag graphene nanoribbon (ZGNR) with widths of 4.26 and 4.92 Å,

respectively. To simulate the dynamics of Ne around clean edges, the AGNR and ZGNR had a hydrogenated edge on one side and a clean edge on the other side. Ne atoms were initially located above alongside or above the clean edge of GNR with a spacing of 3 Å [Fig. 1(a)-**1**(d)]. To simulate the positively charged Ne atoms around graphene edges, we conducted DFT calculations with the aid of the ESM method using the model structure shown in Fig. 1(e), where the Ne and GNRs were located in front of a counter metal electrode simulated by an ESM with an infinite permittivity. The metal electrode was situated at one of the cell boundaries, while an open boundary condition was imposed at the opposite cell boundary by setting the relative permittivity as 1. Accordingly, a positive electric field was applied between the positively charged complexes, comprised of Ne and graphene clean edge, and the negatively charged counter electrode. Integration over the Brillouin zone was carried out using an equidistance mesh of 4 k-points along the edge, which enabled sufficient convergence in the calculation of the total energy and the electronic structures of the GNRs [49]. The three left-most atomic lines (H and C atoms) were fixed during the MD simulations of the Ne atom around the GNR edge under a positive electric field to simulate the infinitely extended graphene networks.

4. Results and discussion

Figure 2 shows the trajectories of Ne atoms around the clean edges of graphene for the first 50 MD steps under a positive electric field at a temperature of 100 and 1000 K. The trajectory of the Ne atom depends on its initial position with respect to the graphene edge and the edge shape. The Ne atom alongside the armchair edge moves directly toward the counter electrode irrespective of the temperature [Fig. 2(a)]. An increase of the temperature simply affected the deviation of the trajectory from the graphene plane, owing to the large thermal fluctuation. In contrast, the Ne atom alongside the zigzag edge approximately stayed around the initial position, even though it experienced a positive electric field with a direction from the edge to the electrode [Fig. 2(b)]. For the cases

where the Ne atoms were situated above the edge C atomic sites, the Ne atom approached graphene layers, irrespective of the edge shape and temperature [Fig. 2(c) and 2(d)]. The MD movie of Ne alongside the armchair edge (Video S1), alongside the zigzag edge (Video S2), above the armchair edge (Video S3) and above zigzag edge (Video S4) under the positive electric field at the temprature of 100K are viewable online. These results indicated that the dynamics of Ne atoms around the graphene edges reflected their local atomic structures. The results also predicted that the FIM images of clean graphene edges were primarily attributed to their armchair portion. Furthermore, the image only contained the edge information but not the in-plane geometric information.

To provide theoretical insight into the dynamics of the Ne atoms around the edges, we investigated the electrostatic potential and electric field around the graphene edges (Fig. 3). For all cases, the electrostatic potential arithmetically increased, which reflected the constant electric field induced by the planar counter electrode on which counter electrons were homogeneous distributed. The potential and electric field reflected the initial position of the Ne atom and edge shapes. For Ne alongside the armchair edge, the potential monotonically decreased with separation from the graphene edge, so that the positively charged Ne atom experienced an attractive force from the negatively charged electrode [Fig. 3(a)]. For Ne alongside the zigzag edge, we found that the potential exhibited a plateau around Ne atom by carefully checking the potential in the vicinity of Ne. This potential plateau was proposed to cause the prowling motion of Ne around the zigzag edge [Fig. 3(b)]. Around the Ne atom above the armchair and zigzag edges [Figs. 3(c) and 3(d)], the direction of the potential gradient or the electric field was normal to the graphene layer. Thus, the Ne above the edge C atomic sites could hardly approach the electrode. The electrostatic potential and electric field could partially explain the dynamics of Ne around the graphene edges. However, it remains uncertain why an attractive trajectory occurred for Ne above the graphene edges.

To deepen the understanding of the dynamics of Ne around the graphene edges, we further evaluated the distribution of the accumulated carriers $\Delta\rho(\vec{r})$

in Ne and GNRs under an external electric field by using the formula,

$$\Delta\rho(\vec{r}) = \rho_q(\vec{r}) - \rho_0(\vec{r}),$$

where $\rho_q(\vec{r})$ and $\rho_0(\vec{r})$ are the valence charge densities with and without the excess holes in the system, respectively. Figure 4 shows the isosurfaces of the accumulated carriers and the corresponding plane-averaged carrier density along the z axis of the GNRs with a Ne atom under a positive electric field. For all cases, the accumulated holes caused by the positive electric field were mainly distributed around the graphene edge and on the Ne atom. However, their detailed distributions depended on the edge shape and the initial position of the Ne atom. For the case where Ne was initially situated alongside the armchair edge, holes were introduced into Ne and the graphene edge. Accordingly, the positively charged Ne experienced a repulsive force from the edge, which resulted in the direct motion of Ne from the edge to electrode. In contrast, when the Ne atom was located alongside the zigzag edge, a dangling bond at the zigzag edge induced polarization on the Ne atom. This induced dipole moment on Ne felt the attractive forces from the edge and electrode, which caused the prowling motion of Ne around the zigzag edge. For the cases of Ne above the edge, polarization was induced on the Ne atom by the accumulated holes around the edges of graphene irrespective of their shapes. Therefore, the dipole on Ne and holes on graphene attractively interacted with each other, which caused the dynamics where the Ne atom approached the graphene layer under the positive electric field. These facts indicated that the complete ionization is the key mechanism to induce the motion of Ne from the graphene edges to the counter electrode.

5. Conclusion

The dynamics of a Ne atom around the clean edges of graphene under a positive electric field were investigated by conducting first-principles MD simulations based on DFT combined with the ESM method. The trajectories for the first 50 MD steps of the Ne atom around the graphene edges strongly depended

on the initial position of the Ne atom and the edge morphology of graphene. The Ne atom rapidly moved toward the electrode when it was initially located alongside a clean armchair edge. The Ne atom nearly maintained its initial position when it was initially located alongside a clean zigzag edge. In contrast, the Ne atom was attracted to the graphene layer when it was initially located above the edge atomic sites. Our analysis on the electrostatic properties reveals that the carrier distribution induced by the field influences the dynamics. For a Ne atom alongside the armchair edge, a repulsive interaction between the positively charged Ne and graphene edge causes a trajectory from the vicinity of the edge to the electrode. While for the remaining cases, the polarization induced on Ne by the injected holes on graphene causes a motion whose direction is opposite to that observed when the Ne is alongside the armchair edge. These results provide theoretical insight into the microscopic mechanism of the field-induced ion dynamics around graphene edges, where the ion is able to detect the detailed atomic arrangement of the clean edges of graphene.

Acknowledgments

This work was supported by JST-CREST Grant Numbers JPMJCR1532 and JPMJCR1715 from the Japan Science and Technology Agency, JSPS KAKENHI Grant Numbers JP20K05664, JP20K22323, JP20K05253, JP20H02080, JP20H00316, JP17H01069 and JP16H06331 from the Japan Society for the Promotion of Science, and the Joint Research Program on Zero-Emission Energy Research, Institute of Advanced Energy, Kyoto University. Part of the calculations was performed on an NEC SX-Ace at the Cybermedia Center at Osaka University.

References

[1] K. S. Novoselov, A. K. Geim, S. V. Morozov, D. Jiang, Y. Zhang, S. V. Dubonos, I. V. Grigorieva, and A. A. Firsov, Science **306**, 666 (2004).

[2] A. K. Geim and K. S. Novoselov, Nat. Mater. **6**, 183 (2007).

[3] I. Forbeaux, J.-M. Themlin, and J.-M. Debever, Phys. Rev. B **58**, 16396 (1998).

[4] C. Berger, Z. Song, X. Li, X. Wu, N. Brown, C. Naud, D. Mayou, T. Li, J. Hass, A. N. Marchenkov, E. H. Conrad, P. N. First, and W. A. de Heer, Science **312**, 1191 (2006).

[5] X. Li, W. Cai, J. An, S. Kim, J. Nah, D. Yang, R. Piner, A. Velamakanni, I. Jung, E. Tutuc, S. K. Banerjee, L. Colombo, and R. S. Ruoff, Science **324**, 1312 (2009).

[6] K. S. Novoselov, A. K. Geim, S. V. Morozov, D. Jiang, M. I. Katsnelson, I. V. Grigorieva, S. V. Dubonos, and A. A. Firsov, Nature **438**, 197 (2005).

[7] Y. Zhang, Y.-W. Tan, H. L. Stormer, and P. Kim, Nature **438**, 201 (2005).

[8] K. I. Bolotin, K. J. Sikes, Z. Jiang, M. Klima, G. Fudenberg, J. Hone, P. Kim, and H. L. Stormer, Solid State Commun. **146**, 351 (2008).

[9] M. Koshino and T. Ando, Phys. Rev. B **76**, 085425 (2007).

[10] S. Konabe and S. Okada, J. Phys. Soc. Jpn. **81**, 113702 (2012).

[11] E. Suárez Morell, J. D. Correa, P. Vargas, M. Pacheco, and Z. Barticevic, Phys. Rev. B **82**, 121407(R) (2010).

[12] R. Bistritzer and A. H. MacDonald, Proc. Natl. Acad. Sci. USA **108**, 12233 (2011).

[13] Y. Cao, V. Fatemi, S. Fang, K. Watanabe, T. Taniguchi, E. Kaxiras, and P. Jarillo-Herrero, Nature **556**, 43 (2018).

[14] M. Otani, M. Koshino, Y. Takagi, and S. Okada, Phys. Rev. B **81** 161403(R) (2010).

[15] Y. Ma, P. O. Lehtinen, A. S. Foster, and R. M. Nieminen, New J. Phys. **6** 68 (2004).

[16] M. Maruyama and S. Okada, Appl. Phys. Express 6, 095101 (2013).

[17] M. Igami, S. Okada, and K. Nakada, Synth. Met. **121**, 1233 (2001).

[18] L. Kong, A. Enders, T. S Rahman, and P. Dowben, J. Phy.: condens. matter **26**, 443001 (2014).

[19] M. Fujita, K. Wakabayashi, K. Nakada, and K. Kusakabe, J. Phys. Soc. Jpn. **65**, 1920 (1996).

[20] K. Nakada, M. Fujita, G. Dresselhaus, and M. S. Dresselhaus, Phys. Rev. B **54**, 17954 (1996).

[21] Y. Miyamoto, K. Nakada, and M. Fujita, Phys. Rev. B **59**, 9858 (1999).

[22] S. Okada and A. Oshiyama, Phys. Rev. Lett. **87**, 146803 (2001).

[23] A. Yamanaka and S. Okada, Carbon **96**, 351 (2016).

[24] M. Maruyama, N. T. Cuong, and S. Okada, Carbon **109**, 755 (2016).

[25] N. Shima and H. Aoki, Phys. Rev. Lett. **71**, 4389 (1993).

[26] M. Ohtsuka, S. Fujii, M. Kiguchi, and T. Enoki, ACS Nano **7**, 6868 (2013).

[27] K. A. Ritter and J. W. Lyding, Nat. Mater. **8**, 235 (2009).

[28] G. M. Rutter, N. P. Guidinger, J. N. Grain, P. N. First and J. A. Stroscio, Phys. Rev B **81**, 245408 (2010).

[29] J. F. Tian, H. L. Cao, W. Wu, Q. K. Yu and Y. P. Chen, Nano Lett. **11**, 3663 (2011).

[30] Ç. Ö. Girit, J. C. Meyer, R. Erni, M. D. Rossell, C. Kisielowski, L. Yang, C. H. Park, M. F. Crommie, M. L. Cohen, S. G. Louie, and A. Zettl, Science **323**, 1705 (2009).

[31] K. Nakakubo, K. Asaka, H. Nakahara, and Y. Saito, Appl. Phys. Express **5**, 055101 (2012).

[32] C. Wang, H. Nakahara, and Y. Saito, Surf. Interface Anal. **48**, 1221 (2016).

[33] N. Yokoyama, K. Nakakubo, K. Iwata, K. Asaka, H. Nakahara, and Y. Saito, Surf. Interface Anal. **48**, 1217 (2016).

[34] Y. Saito, R. Mizushima, and Junko, and K. Hata, Surf. Sci. Lett. **499**, L119 (2002).

[35] D. Lovall, M. Buss, E. Graugnard, R. P. Andres, and R. Reifenberger, Phys. Rev. B **61**, 5683 (2000).

[36] T. I. Mazilova, I. M. Mikhailovskij, V. A. Ksenofontov, and E. V. Sadanov, Nano Lett. **9**, 774 (2009).

[37] C. Barroo and T. V. de Bocarmé, Microsc. Microanal. **22**, 1542 (2016).

[38] K. Tada and K. Watanabe, Phys. Rev. Lett. **88**, 127601 (2002).

[39] Y. Gao and S. Okada, Carbon **157**, 33 (2020).

[40] Y. Gao and S. Okada, Carbon **142**, 190 (2019).

[41] Y. Gao and S. Okada, Appl. Phys. Lett. **112**, 163105 (2018).

[42] P. Hohenberg and W. Kohn, Phys. Rev. **136**, B864 (1964).

[43] W. Kohn and L. J. Sham, Phys. Rev. **140**, A1133 (1965).

[44] Y. Morikawa, K. Iwata, and K. Terakura, Appl. Surf. Sci. **169-170**, 11 (2001).

[45] J. P. Perdew and A. Zunger, Phys. Rev. B **23**, 5048 (1981).

[46] D. M. Ceperley and B. J. Alder, Phys. Rev. Lett. **45**, 566 (1980).

[47] S. Okada, S. Saito, and A. Oshiyama, Phys. Rev. Lett. **86**, 3835 (2001).

[48] D. Vanderbilt, Phys. Rev. B **41**, 7892(R) (1990).

[49] A. Yamanaka and S. Okada, Carbon **96**, 351 (2006).

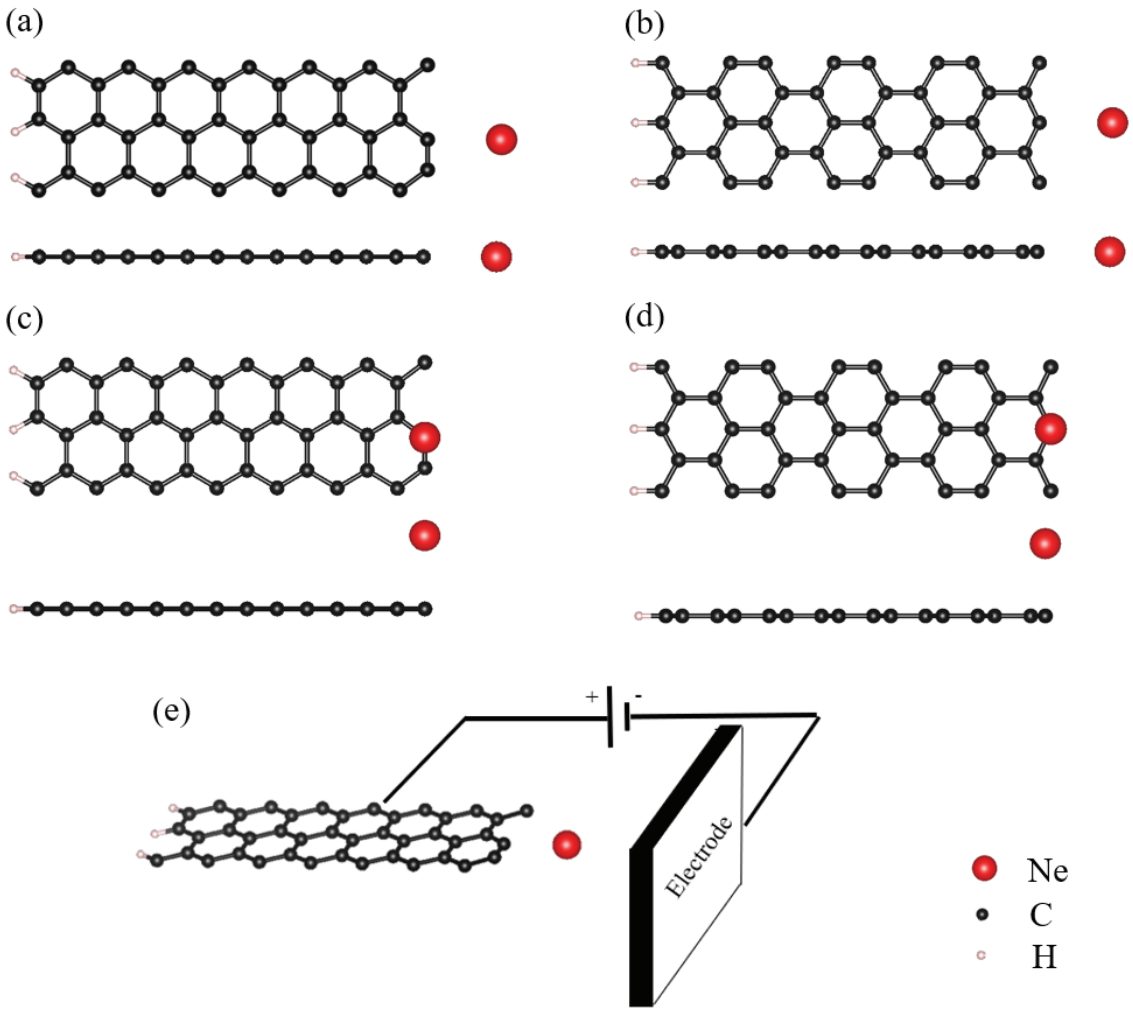

Figure 1: Geometric structures of (a) AGNR and (b) ZGNR with a Ne atom alongside their clean edges, and those of (c) AGNR and (d) ZGNR with a Ne atom above their edge atomic site. (e) A structural model to simulate a Ne atom around the graphene edges under a positive electric field. Holes are injected into Ne and GNR via the counter electrode denoted by the marked slab on the right of the figure. Gray, red, and white balls indicate C, Ne, and H atoms, respectively.

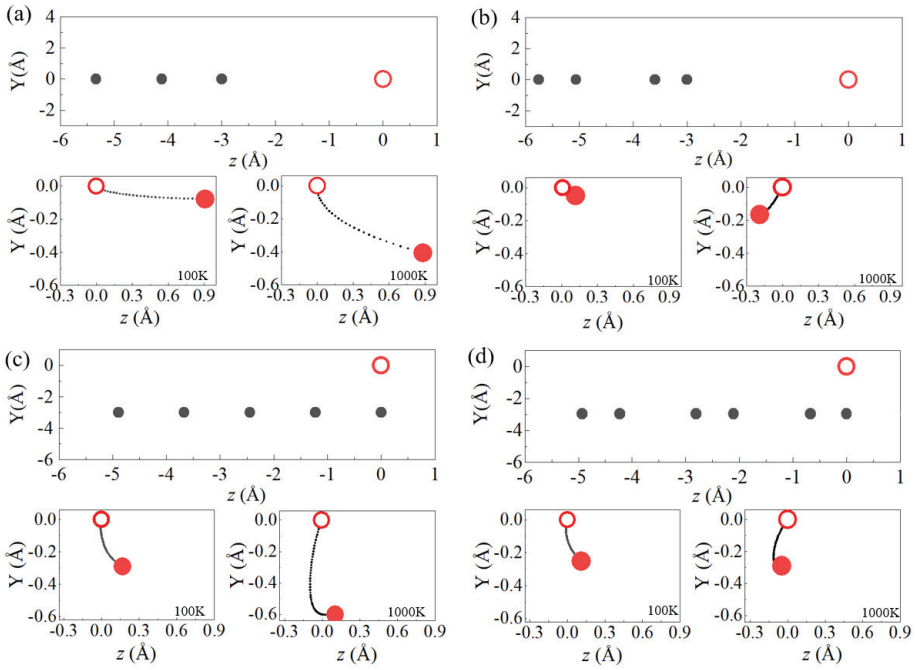

Figure 2: MD trajectories of a Ne atom (a) alongside the armchair edge, (b) alongside the zigzag edge, (c) above the armchair edge, and (d) above the zigzag edge after the first 50 MD steps. Top panel in each figure indicates the initial atomic arrangement of the CNR with Ne, where black filled and red open circles denote the C and Ne atoms, respectively. Bottom two panels in each figure show the trajectory under a temperature of 100 and 1000 K. Red open and filled circles indicate the initial and final position of Ne under the MD, respectively.

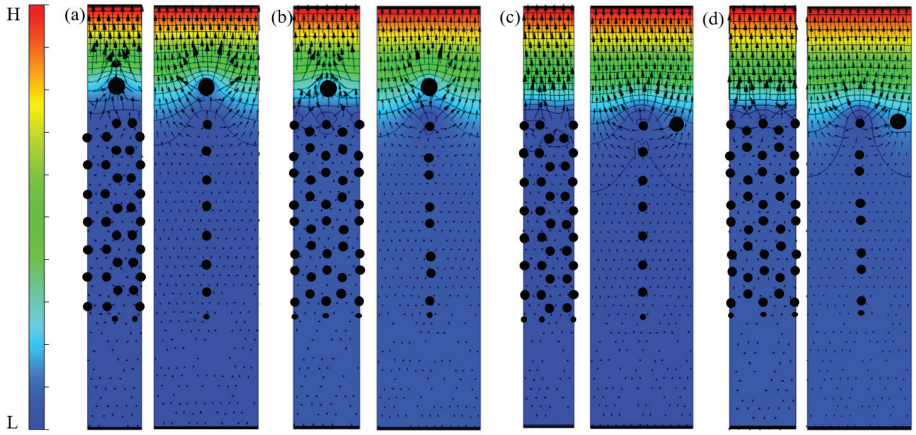

Figure 3: Contour and vector plots of the electrostatic potential and electric field of GNRs with a Ne atom, whose position is (a) alongside the armchair edge, (b) alongside the zigzag edge, (c) above the armchair edge, and (d) above the zigzag edge, on the plane parallel and normal to the graphene layers. Black circles denote the atomic positions.

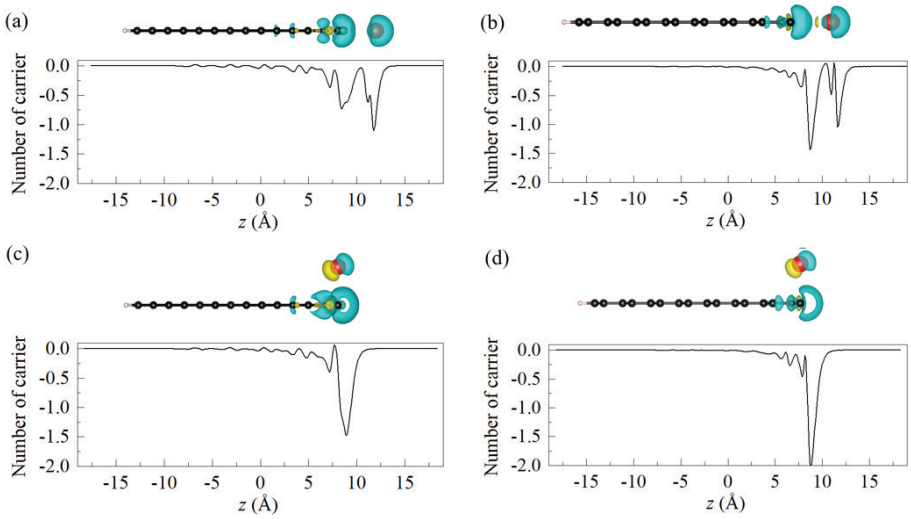

Figure 4: Isosurfaces of an accumulated hole $\Delta\rho(\vec{r})$ and plane-averaged accumulated hole as a function of z of GNRs with Ne (a) alongside the armchair edge, (b) alongside the zigzag edge, (c) above the armchair edge, and (d) above the zigzag edge. The cyan and yellow colors indicate accumulated holes and electrons with a isosurface value of 0.013 /Å^3, respectively.